Chemical Physics 355 (2009) 183–193

Contents lists available at ScienceDirect

Chemical Physics

journal homepage: www.elsevier.com/locate/chemphys

Threshold photoelectron spectroscopy of H_2O and D_2O over the photon energy range 12–40 eV

S.Y. Truong [a,1], A.J. Yencha [b,*], A.M. Juarez [c], S.J. Cavanagh [a,2], P. Bolognesi [d], G.C. King [a]

[a] School of Physics and Astronomy, The University of Manchester, Manchester M13 9PL, United Kingdom
[b] Department of Chemistry, State University of New York at Albany, Albany, NY 12222, USA
[c] Instituto de Ciencias Físicas, Universidad Nacional Autónoma de México, P.O. Box 48-3, Cuernavaca 62251, Mor., Mexico
[d] CNR-IMIP, Area della Ricerca di Roma 1, CP10 00016 Monterotondo Scalo, Rome, Italy

ARTICLE INFO

Article history:
Received 29 May 2008
Accepted 5 December 2008
Available online 13 December 2008

Keywords:
Threshold photoelectron spectroscopy
Photoionization of water
Synchrotron radiation

ABSTRACT

The threshold photoelectron spectra of H_2O and D_2O have been recorded over the ionization region (12–40 eV) under high-resolution conditions using synchrotron radiation. Extensive vibrational 'filling-in' is found in the Franck–Condon gap regions between the three lowest ionic-state band systems that is attributed to autoionization of Rydberg states lying in these binding-energy regions. Vibronic coupling effects are found in the A $^2A_1$ band system of H_2O^+ and D_2O^+ in general agreement with a previous experiment. An unusual intensity enhancement is found in the B $^2B_2$ band system in the threshold photoelectron spectra of H_2O and D_2O that is attributed to an enhanced production of H_2O^+ and D_2O^+ ions due to the autoionization of Rydberg states lying in the binding energy region of this electronic state. In the inner valence ionization region two broad features have been found that are attributed to the $(2a_1)^{-1}$ 'main-line' state and the $(1b_1)^1 4a_1^*$ resonant state.

1. Introduction

The study of water (H_2O) is of great interest as it is one of the most abundant substances on the Earth's surface and is a major constituent of all living organisms. It is also an important constituent of the Earth's atmosphere and is found in many forms in the cosmos, such as in comets, throughout galaxies, and in the general interstellar space. In this regard, the interaction of ultraviolet radiation with water is of particular interest as it can be ionized forming H_2O^+, which is in itself an important species in the cosmos.

The electronic states of H_2O^+ have been studied for a very long time and by many methods and techniques dating back to the mid-1930s [1,2]. However, the greatest amount of knowledge about the ionic states of H_2O comes from photoelectron spectroscopy (PES) using the HeI light source. A few examples of such measurements include Al-Joboury and Turner [3], Brundle and Turner [4], Potts and Price [5], Karlsson et al. [6] and Dixon et al. [7]. These early photoelectron measurements of H_2O^+ were able to detect the first three states of the ion, for which the respective adiabatic and vertical ionization potentials were measured. Brundle and Turner [4] first attempted to assign the vibrational structure of the three lowest ionic states of H_2O. Using a HeI photon source, they obtained photoelectron spectra of H_2O and D_2O, with a resolution of approximately 20 meV. For the ground ionic state (X $^2B_1$), the position of the adiabatic potential energy was clearly seen and was measured to be 12.61 eV. They also assigned a combination of the normal vibrations ν_1 and ν_2, to the relatively short vibrational progression of the ionic ground state. The second ionic state (A $^2A_1$), was assigned to have a progression in just one frequency, ν_2. However the position of the adiabatic potential was not clear. A value of 13.7 eV was obtained by extrapolating their data. Proper assignment of the more complex third ionic state was not made, but an extrapolated value for the adiabatic potential energy was found to be 17.22 eV. Building on the work of Brundle and Turner [4], Karlsson et al. [6] and Dixon et al. [7] attempted to re-assign the vibrational progressions of these three ionic states, using their higher resolution PE data. However, their assignments do not agree with each other. Karlsson et al. also calculated values of the force constants for H_2O^+ in the X $^2B_1$ state.

In addition to photoelectron measurements, electron impact studies of the ionic states of water has been carried out, one of the more recent of which was by Lew [8]. Lew looked at the emission spectrum of H_2O^+, obtained from the transition A $^2A_1 \rightarrow$ X $^2B_1$, and from the data was able to assign rotational constants for the states involved. Lew also measured the O–H bond length and the H–O–H angle for the X $^2B_1$ state. More recently, Leclerc et al. [9] and Jackels [10] carried out theoretical studies of the electronic states of H_2O^+ using configuration interaction (CI) techniques. This

---

* Corresponding author. Tel./fax: +1 518 442 3462.
E-mail address: yencha@albany.edu (A.J. Yencha).

[1] Present address: Waters, Altrincham, Cheshire WA14 5RZ, United Kingdom.

[2] Present address: Research School of Physical Sciences and Engineering, The Australian National University, Camberra 0200, Australian Capital Territory, Australia.

0301-0104/$ - see front matter © 2008 Elsevier B.V. All rights reserved.
doi:10.1016/j.chemphys.2008.12.009

allowed the molecular structure of the three lowest ionic states to be calculated, as well as their dissociation paths.

In the present work the singly ionized valence states of H_2O and D_2O were studied using high-resolution threshold photoelectron spectroscopy (TPES). To our knowledge and amazement, full TPE spectra of the valence states of H_2O and D_2O have not been published previously, although a preliminary report on the TPE spectra of the outer valence states of H_2O and D_2O was given in an abstract of a paper presented at an international conference [11]. In addition, we have obtained the medium-resolution PE spectrum of H_2O for a direct comparison with the TPE spectrum of H_2O.

2. Experimental

The electron spectra of H_2O and D_2O reported here were recorded at the Synchrotron Radiation Source (SRS) facility of the Daresbury Laboratory (UK) on two different beamlines (3.2 and 3.3) incorporating two different monochromators (a 5-m McPherson normal incidence monochromator and a toroidial grating monochromator, respectively). The apparatus used on both beamlines was a purpose built electron spectrometer system for measuring threshold photoelectrons coincidence (TPEsCO) spectra in photo-double ionization of atomic and molecular systems [12]. It consists of two identical 127° electron energy analyzers mounted on separate concentric turntables. The analyzers are mounted so that the axis of the lens stack within each analyzer is perpendicular to and centered about the axis of the photon beam. The gas is delivered into the experimental chamber through a 1.0 mm bore molybdenum gas needle, which is attached to a *xyz*-manipulator situated on top of the chamber and 12 mm from the entrance lens of each analyzer. The gas needle sits perpendicular to the axis of each lens stack and the photon beam. The end of the gas needle is position approximately 2 mm above the top of the photon beam. To reduce any stray magnetic fields that might be present, a pair of mu-metal shields surrounds the spectrometer. The chamber and gas inlet lines are heated to 50–60 °C as a means of stabilizing and improving the performance of the electron spectrometer.

In the experiments described here only one of the electron energy analyzers was used. The other one was turned off. The analyzer could be operated in either the constant-kinetic-energy mode or in the threshold mode. In the constant-kinetic-energy photoelectron spectroscopy (CKE-PES) mode, the analyzer collection energy is set to the fixed value of 0.5 eV while the photon energy is increased in uniform steps over the required energy range. In this mode of collection the electron energy analyzer is fixed in position at an angle of 0° with respect to the plane of the polarization vector of the radiation. Since the measurements were not obtained at the "magic angle" the observed intensities are influenced by the angular distributions of the photoelectrons. However, this does not affect the present spectroscopic analysis of the observed spectra. The overall energy resolution of the CKE-PES spectrum depends on the resolution of the analyzer and the energy spread of the photon beam. Moreover, the photoelectrons are collected over a finite solid angle ($\sim 10^{-2}\pi$ sr) that is determined by the diameter of the entrance aperture of the analyzer.

In the threshold mode of operation, a voltage (typically 70–100 V) is applied to the first (extractor) lens so as to provide an extraction field in the interaction region. This is known as the *penetrating-field technique*, as described by Cvejanović and Read [13]. The field has the effect of enhancing the extraction efficiency of threshold photoelectrons by re-directing electrons that are initially not travelling in the direction of the analyzer, towards the analyzer. This technique allows for the efficient collection of threshold electrons, which have energies of ~0–10 meV (although ~95% of the electrons collected are within 3 meV of threshold), over a large solid angle ($\approx 4\pi$ sr). Higher energy electrons, which are not travelling in the direction of the analyzer, cannot be trapped by the relatively weak field and so are not collected. The high-energy electrons traveling in the direction of the analyzer are removed from detection by the 127° electrostatic analyzer that acts as a filter.

In this mode of operation the collection energy of the electrons is kept constant (near zero energy) while the photon energy is increased over the required energy range. A zero-energy electron is produced whenever the photon energy scans across a threshold for the production of an ion. A TPE spectrum therefore measures the binding energies of the electrons in a molecule, or the energies of any other process that produces zero-energy electrons. For this mode of collection the overall energy resolution depends essentially only on the resolution of the photon energy, and resolutions of a few meV are possible [14]. With this method, because the photon energy is varied it is possible that the photon energy coincides with the excitation energy of Rydberg states. These excited states could then also produce threshold electrons by autoionizing to ionic states lying slightly below them in energy.

For both beamlines, the light from the monochromator is transported to the experimental apparatus through a Pyrex capillary with a bore diameter of 1.0 mm. The capillary allows for differential pumping between the relatively high pressure of the apparatus ($\sim 10^{-5}$ mbar) and the relatively low pressure in the monochromators ($\sim 10^{-9}$ mbar).

The method of recording threshold photoelectron (TPE) spectra by the *penetrating-field technique* has been given in detail before [15] so only a brief description will be given here. The spectrometer was tuned to detect near-zero energy electrons using the argon-ion doublet lines at 15.759 eV ($^2P_{3/2}$) and 15.937 eV ($^2P_{1/2}$). Photon energy calibration was achieved by measuring the TPE spectra of the rare gases He through Xe and the TPE spectrum of the satellite states of Ar extending up to approximately 40 eV.

The TPE spectra of H_2O and D_2O were recorded on beamline 3.2 (McPherson monochromator) over the binding energy range 12–40 eV that encompasses both the outer and inner valence ionization regions in the molecules. The H_2O TPE spectrum presented here is the sum of four scans. The four separate spectra were collected in 7 meV steps with a 5 s dwell time per step. Each scan was intensity normalized for the time decay of the synchrotron light before summing. The same procedure was used to obtain the D_2O TPE spectrum presented here by summing three separate scans. The three spectra were collected in 7 meV steps with a 3 s dwell time per step and intensity normalized for the decay of the synchrotron light in time before summing. The resolution of both presented TPE spectra is ~8 meV at 15.759 eV ($E/\Delta E \approx 2000$). In addition, the (0.5 eV) constant-kinetic-energy photoelectron (PE) spectrum of H_2O was recorder on beamline 3.3 (toroidial grating monochromator) over the binding energy range 12–20.5 eV. The final presented PE spectrum is a sum of four separate scans that were intensity normalized for the time decay of the synchrotron light before summing. Each spectrum was collected with a photon energy step size of 5 meV and a dwell time of 5 s per step. The final PE spectrum was corrected for the transmission function of the energy analyzer. This medium-resolution PE spectrum was recorded as a means for a direct comparison with the TPE spectrum of H_2O.

3. Results and discussion

3.1. General considerations

H_2O is a non-linear, triatomic molecule consisting of an oxygen atom covalently bonded to two hydrogen atoms. The ground state of the H_2O molecule is classified as belonging to the C_{2v} point group and so the electronic states of water are described using the irreducible representations A_1, A_2, B_1 and B_2. The electronic configuration of the ground state of the H_2O molecule is described by five doubly occupied molecular orbitals [16]:

$$\underbrace{(1a_1)^2}_{\text{core}} \qquad \underbrace{(2a_1)^2}_{\substack{\text{inner - valence}\\ \text{orbital}}} \qquad \underbrace{(1b_2)^2\,(3a_1)^2\,(1b_1)^2}_{\substack{\text{outer - valence}\\ \text{orbitals}}} \qquad X\,{}^1A_1$$

The H_2O molecule possesses three normal modes of vibration. They are the symmetric stretch (ν_1), the symmetric bend (ν_2) and the antisymmetric stretch (ν_3). The vibrational energies corresponding to the normal modes of the ground state of H_2O and D_2O are given in Table 1.

The complete TPE spectrum measured for H_2O, spanning the photon energy region 12–40 eV, is shown in upper panel of Fig. 1. In addition to the three band systems observed in HeI PES of H_2O [3–7], a fourth band system in the TPE spectrum close to 32 eV is also observed. As indicated in Fig. 1, these band systems correspond to the removal of a valence electron from each of the molecular orbitals $(1b_1)^{-1}$, $(3a_1)^{-1}$, $(1b_2)^{-1}$and $(2a_1)^{-1}$ of H_2O. The first three band systems, corresponding to the formation of the X $^2B_1$, A $^2A_1$ and B $^2B_2$ ionic states of H_2O, respectively, all show resolved vibrational structure. The fourth band system does not appear to have any vibrational structure associated with it but it does have a low-energy shoulder that also appears structureless. The corresponding TPE spectrum of D_2O is shown in the lower panel of Fig. 1. As would be expected, the band systems observed are very similar to those found in the TPE spectrum of H_2O, except for the smaller vibrational separations in the first three band systems of D_2O due to the isotope effect.

3.2. Overview of outer valence ionization region in H_2O

The (0.5 eV) constant-kinetic-energy PE spectrum of H_2O covering the binding energy region, 12–20.5 eV, of the three outer valence states of H_2O^+ (X $^2B_1$, A $^2A_1$ and B $^2B_2$) is shown in lower panel of Fig. 2 where it is directly compared to the corresponding region in the TPE spectrum of H_2O in the upper panel. There are several differences in the general features of the two spectra. The first and most obvious difference is in the sudden increase in the photoelectron yield within the third band system in the TPE spectrum at ~18.1 eV. A similar abrupt increase in the photoelectron yield in the third band system is observed in the TPE spectrum of D_2O (see Fig. 1) at ~18.2 eV. Another difference between the TPE and PE spectra of H_2O is the 'filling-in' in between the band systems in the TPE spectrum. This is a common feature in TPE spectra and is due to the presence of Rydberg states lying in between adjacent ionic states (in the Franck–Condon gap region) [18]. These Rydberg states can autoionize into higher vibrational levels of the lower energy electronic state that are in resonance with the Rydberg levels, thus producing threshold electrons, that are detected. A third difference to be noted between the TPE and PE spectra of H_2O is the shifting to lower energy of the maximum intensity in the second and third band systems in the TPE spectrum. This is most clearly seen in the second band system, but it is also observed to a lesser extent in the third band system. Other differences to be noted are the much higher resolution achieved in the TPE spectrum and the enhanced yield (20 times greater) of photoelectrons in TPE spectrum. We will comment more about some of these differences when we discuss the individual band systems in the TPE spectra of H_2O and D_2O.

Table 1
Energies (in meV) of the normal modes of vibration for the $^1A_1$ ground state of H_2O and D_2O.

Molecule	Normal vibrational mode energy		
	Symmetric stretch, $h\nu_1$	Symmetric bend, $h\nu_2$	Antisymmetric stretch, $h\nu_3$
H_2O[a]	453	198	466
D_2O[b]	331	146	345

[a] Herzberg [17].

[b] Karlsson et al. [6].

To analyze the vibrational structure of each electronic band of H_2O^+ and D_2O^+, initially the assignments of Karlsson et al. [6] were used as a guide to assign the first few vibrational levels in each band. This allowed the energy values for the normal modes of vibration (ν_1, ν_2 and ν_3) to be determined. Knowing the values of these vibrational energies for each ionic state from the TPE data, a fuller assignment was made. This was done by extrapolating the energies of the normal vibrations in the region of interest, and allowed estimates of the positions of other possible vibrational levels. The four bands seen in the upper and lower panels of Fig. 1 for H_2O^+ and D_2O^+, respectively, have been analyzed individually.

3.3. Vibrational analysis of the H_2O^+ and D_2O^+ (X $^2B_1$) band systems in the TPE spectra

In upper panel of Fig. 3 is shown an expanded view of the first band in the TPE spectrum of H_2O, corresponding to the X $^2B_1$ state of H_2O^+. The vibrational structure of this band is characteristic of ionization from a non-bonding molecular orbital. The extent of vibrational structure of this band is relatively slight, with a very sharp and intense peak (at the beginning of the band) corresponding to the transition $^2B_1$ (0,0,0) ← $^1A_1$ (0,0,0), i.e. from the neutral molecular ground state to the ground state of H_2O^+. This transition gives the position of the adiabatic ionization energy of the X $^2B_1$ state of H_2O^+ to be 12.621 ± 0.008 eV. This compares well with the values of 12.61 eV, 12.615 eV and 12.624 eV, obtained by Brundle and Turner [4], Karlsson et al. [6] and Dixon et al. [7], respectively. Because the peak corresponding to the adiabatic transition is the most intense peak, it also corresponds to the vertical ionization energy of the state. The lower panel of Fig. 3 shows the corresponding band system of D_2O^+. As expected, the structure of the band is similar to that of H_2O^+. The adiabatic ionization energy of the X $^2B_1$ state of D_2O^+ is measured to be 12.641 ± 0.008 eV. This compares well with the values of 12.62 eV, 12.633 eV and 12.637 eV, measured by Brundle and Turner [4], Karlsson et al. [6] and Dixon et al. [7], respectively.

Vibrational analysis of the structure in the first band system in the TPE spectra of H_2O and D_2O was accomplished by reference to the work of Karlsson et al. [6] from which the energies of the normal modes of vibration ν_1 and ν_2 were determined to be 405 meV and 178 meV, respectively, for the X $^2B_1$ state of H_2O^+ and 294 meV and 133 meV, respectively, for the X $^2B_1$ state of D_2O^+. Knowing the values of ν_1 and ν_2, the force constants k_1 and k_δ/l^2 could be calculated using the valence-force approximation [19]. The calculated values of these force constants using a bond angle (2α) of 108.2° [6] are given in Table 2 where they are compared with those of Karlsson et al. [6]. Knowing the value of the force constant k_1, the energy value of the third normal mode of vibration ν_3 could be calculated [19]. The energies of the normal modes of vibration for the X $^2B_1$ state of H_2O^+ and D_2O^+ thus obtained are presented in Table 3 together with the values obtained by Karlsson et al. [6]. As can be seen there is good agreement between the present work and that of Karlsson et al. [6]. Using the vibrational energies from the present work a vibrational assignment was made of the X $^2B_1$ state of H_2O^+ and D_2O^+, as shown in the upper and lower panels

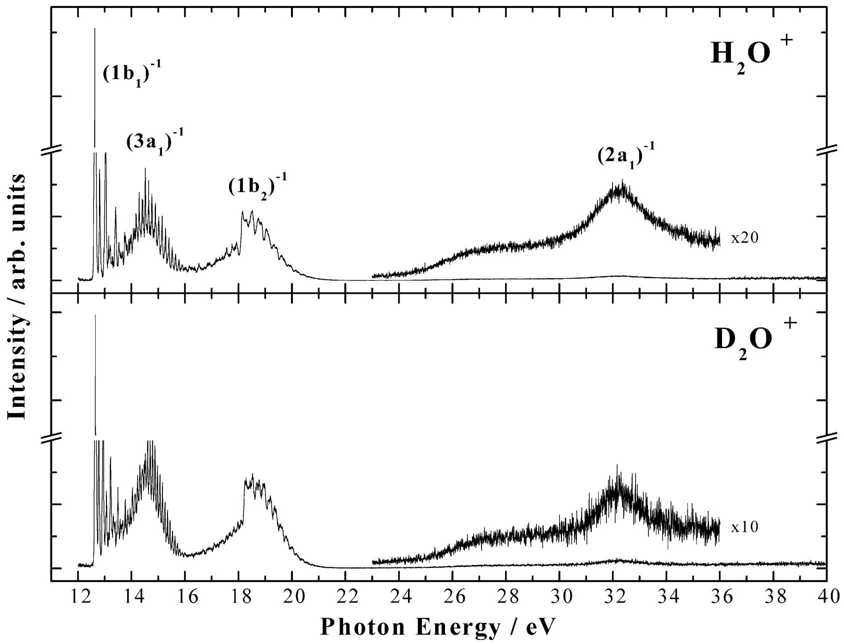

Fig. 1. Complete TPE spectra of H_2O and D_2O over the binding energy region 12–40 eV. The four valence bands $(1b_1)^{-1}$, $(3a_1)^{-1}$, $(1b_2)^{-1}$ and $(2a_1)^{-1}$ are shown.

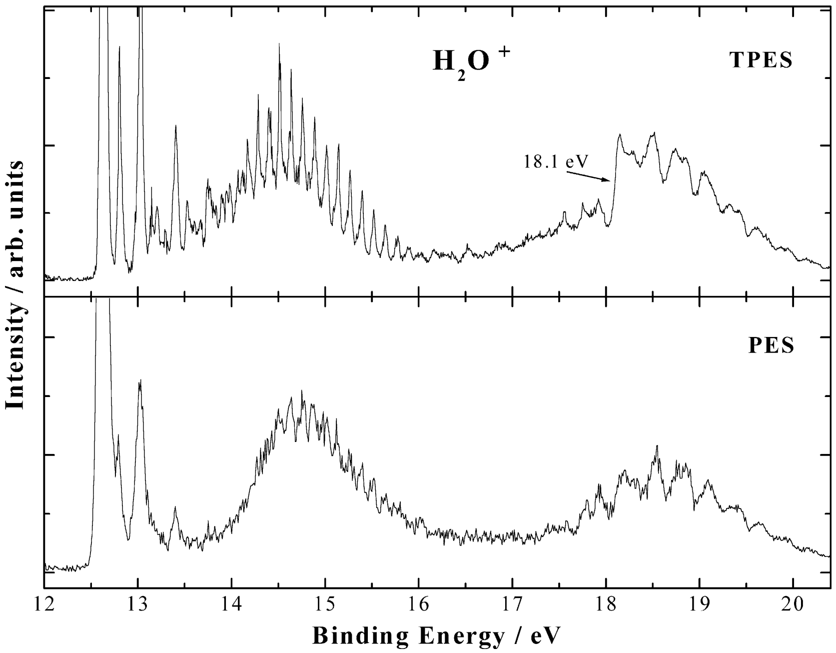

Fig. 2. Comparison between the TPE spectrum of H_2O and the (0.5 eV) constant-kinetic-energy PE spectrum of H_2O over the binding energy region 12–20.5 eV showing the X $^2B_1$, A $^2A_1$ and B ^{2} B_2 band systems of H_2O^+. The yield of photoelectrons using the TPES method is approximately 20 times greater than the yield of photoelectrons using the PES method. Note the sudden increase in intensity at ~18.1 eV and beyond in the TPE spectrum.

of Fig. 3, respectively, and reported in Tables 4 and 5, respectively, where the present results are compared with the previous work of Karlsson et al. [6] and Dixon et al. [7]. As can be seen from these figures and tables far more vibrational levels are assigned in the present work, including the identification of four vibrational progressions, $n\nu_1$, $n\nu_2$, $n\nu_1 + \nu_2$ and $\nu_1 + n\nu_2$, instead of just two progressions previously reported [4,6,7]. We attribute the observation of additional vibrational levels to firstly the high-resolution (6 meV at 12 eV photon energy) of the current study and secondly to the indirect populating of vibrational levels due to autoionization processes.

3.4. Vibrational analysis of the H_2O^+ and D_2O^+ (A $^2A_1$) band systems in the TPE spectra

The upper and lower panels of Fig. 4 show expanded views of the second band system in the TPE spectra of H_2O and D_2O, respectively. This band system corresponds to the ejection of an electron from the $3a_1$ molecular orbital. The band is very broad in extent with what appears, on first sight, to be made up of a simple regular vibrational structure. Previous early photoelectron reports on water [4,6,7] suggested that the vibrational structure consist of a single progression in the vibrational mode ν_2, although Karlsson

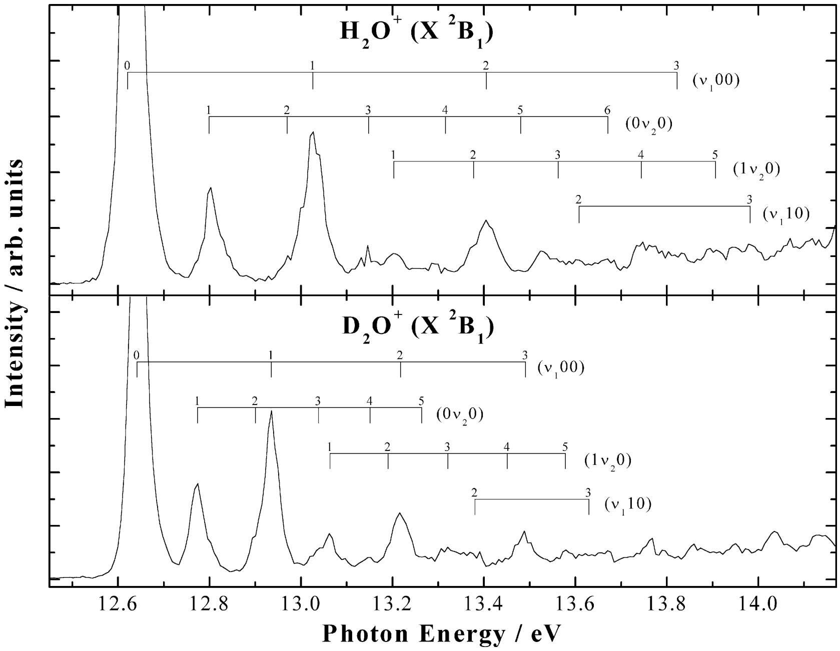

Fig. 3. Expanded views of a portion of the TPE spectra of H_2O and D_2O covering the X $^2B_1$ band system of H_2O^+ and D_2O^+ at an estimated energy resolution of ~6 meV. The spectra were recorded in 7 meV steps.

et al. [6] did note a second progression at the high energy limit of the band system that was suggested could be a combination of ν_1 and ν_2 excitations. More recently in a rotationally-cooled HeI photoelectron study of H_2O and D_2O [20] two vibrational progressions were identified over the entire band system; they being the ν_2 normal mode and the combination progression $\nu_1 + n\nu_2$. In the case of the ν_2 progression, due to vibronic coupling as a result of the Renner–Teller effect, each vibrational band was found to be split into vibronic sublevels. This comprehensive assignment was used as an aid in the present analysis of the $^2A_1$ band system in the TPE spectra of H_2O and D_2O. Although the positions of some of the vibrational peaks in the present study do not match perfectly those measured by Reutt et al. [20], this is understandable because the present data were not obtained with rotationally cooled sources. In addition, in some places the present data may look distorted due to the fact that the envelope of the vibrational peaks consists of rotational structure. The vibrational assignment for the A $^2A_1$ state of H_2O^+ and D_2O^+ from the present data are given in Table 6. In assigning the TPE data, some of the gaps in the vibrational progressions of Reutt et al. [20] for both gases have been filled in. From the present data, the average value of the splitting between the Σ and Δ vibronic states was measured to be ~14 meV and for the Π and Φ vibronic states a splitting of ~23 meV was found. These values are consistent with the values of 14.8 meV for the Σ and Δ vibronic states and ~28 meV for the Π and Φ vibronic states obtained by Reutt et al. [20].

By comparing the TPE spectrum of H_2O^+ with that of D_2O^+, the positions of the adiabatic ionization energies for the A $^2A_1$ state

Table 2
Comparison between calculated values of the force constants (in 10^5 dynes/cm) for the X $^2B_1$ state of H_2O^+ and D_2O^+ with previous work.

Force constant	Present work		Previous work[a]	
	H_2O^+	D_2O^+	H_2O^+	D_2O^+
k_1	5.93 ± 0.47	6.00 ± 0.25	5.93 ± 0.04	6.04 ± 0.05
k_δ/l^2	0.56 ± 0.11	0.56 ± 0.11	0.56 ± 0.03	0.58 ± 0.02

[a] Karlsson et al. [6].

Table 3
Comparison between measured energies (in meV) of the ν_1 and ν_2 normal vibrational modes and calculated energy of the ν_3 normal vibrational mode of the X $^2B_1$ state of H_2O^+ and D_2O^+ with previous work.

Normal modes	Vibrational energy			
	Present work		Previous work[a]	
	H_2O^+	D_2O^+	H_2O^+	D_2O^+
$h\nu_1$	405 ± 10	294 ± 10	402 ± 2	293 ± 2
$h\nu_2$	178 ± 10	133 ± 10	177 ± 2	132 ± 2
$h\nu_3$	409 ± 4	302 ± 8	409	303

[a] Karlsson et al. [6].

Table 4
Ionization energies (I.E.) (in eV) and vibrational assignments of the X $^2B_1$ state of H_2O^+ for this work in comparison with previous works.

Vibrational assignment ($\nu_1\,\nu_2\,\nu_3$)	Present work		Previous works	
	I.E.[a]	Intensity	I.E.[b]	I.E.[c]
000	12.621	1.000	12.615	12.624
010	12.799	0.127	12.792	12.797
020	12.970	0.037		12.960
100	13.026	0.201	13.017	13.021
030	13.148	0.052		13.121
110	13.203	0.041	13.191	13.191
040	13.316	0.022		
120	13.377	0.050		13.354
200	13.405	0.085	13.408	13.406
050	13.480	0.043		
130	13.562	0.033		
210	13.608	0.032	13.578	13.567
060	13.671	0.031		
140	13.744	0.052		
300	13.822	0.040	13.787	13.784
150	13.906	0.046		
310	13.982	0.053		

[a] Uncertainty ±0.008 eV.
[b] Karlsson et al. [6].
[c] Dixon et al. [7].

Table 5

Ionization energies (I.E.) (in eV) and vibrational assignments of the X $^2B_1$ state of D_2O^+ for this work in comparison with previous works.

Vibrational assignment ($v_1 v_2 v_3$)	Present work		Previous works	
	I.E.[a]	Intensity	I.E.[b]	I.E.[c]
000	12.641	1.000	12.633	12.637
010	12.774	0.198	12.765	12.768
020	12.900	0.091		
100	12.935	0.293	12.926	12.928
030	13.038	0.066		
110	13.063	0.084	13.054	13.053
040	13.151	0.046		
120	13.190	0.072		
200	13.217	0.125	13.211	13.210
050	13.264	0.046		
130	13.321	0.066		
210	13.380	0.055	13.211	13.339
140	13.451	0.045		
300	13.491	0.099	13.491	13.486
150	13.578	0.056		
310	13.629	0.043	13.618	

[a] Uncertainty ±0.008 eV.

[b] Karlsson et al. [6].

[c] Dixon et al. [7].

of both molecules can be estimated. As expected, the feature corresponding to the 0-0 transition for both molecules nearly coincides in energy, apart from the isotopic difference of zero-point energies. For H_2O the value of the adiabatic ionization energy was deduced to be 13.748 ± 0.008 eV, and for D_2O a value of 13.768 ± 0.008 eV was obtained. As expected, these values are very similar and the difference between these values is ~20 ± 10 meV. Since the difference in the adiabatic energies obtained for the X $^2B_1$ state of H_2O^+ and D_2O^+ was also determined to be equal to 20 ± 10 meV, this supports the values of the adiabatic energies obtained for the A $^2A_1$ state, measured from the present work. For the A $^2A_1$ state of H_2O^+, the adiabatic energy (13.748 ± 0.008 eV) compares reasonably well with the extrapolated value of 13.7 eV obtained by Brundle and Turner [4] but differs substantially from the value of 13.839 eV reported by Karlsson et al. [6] based on their identification of the first band in the vibrational progression. Also, the feature chosen to be the 0-0 peak in the current work lies approximately one quantum of ν_2 lower than the peak assigned to the (0 1 0) state by Reutt et al. [20].

An estimate for the energy of the ν_2 mode can be obtained by calculating the difference between the states with $\nu_2 = 1$ and $\nu_2 = 2$. A value of $\nu_2 = \sim 112 \pm 10$ meV is obtained for the A $^2A_1$ state of H_2O^+, which is lower than the value for the ground state of the neutral molecule and is consistent with the ionization of a bonding electron. Similarly for the A $^2A_1$ state of D_2O^+, an estimated value of $\nu_2 = \sim 57 \pm 10$ meV is obtained. An estimate for the energy of the ν_1 mode can be obtained by calculating the combination difference between the (1 16 0) and (0 16 0)-Φ states. A value of $\nu_1 = \sim 391 \pm 21$ meV is thus obtained for the A $^2A_1$ state of H_2O^+. This value is similar to the value of 385.7 meV reported by Reutt et al. [20] for the same vibrational levels. Similarly for the A $^2A_1$ state of D_2O^+, an estimated value of $\nu_1 = \sim 303 \pm 10$ meV is obtained from combination differences between the (1 ν_2 0) and (0 ν_2 0) states for values of $\nu_2 = 12$ and 13. This is similar to the value of 313.8 meV reported by Reutt et al. [20]. Using the values of ν_1 and ν_2 obtained here an approximation of the values for the force constants (k_1 and k_δ/l^2) and ν_3 can be made using a linear geometry ($2\alpha = 180°$) [19]. The results for both H_2O and D_2O are reported in Table 7. To the authors' knowledge no calculations exist, from previous experiments, of the values of the ν_3 normal vibrational mode energies and force constants for this state.

3.5. Vibrational analysis of the H_2O^+ and D_2O^+ (B $^2B_2$) band systems in the TPE spectra

The upper panel of Fig. 5 shows an expanded view of the B $^2B_2$ band system of H_2O^+. This band is quite broad, with a sharp increase in the threshold photoelectron intensity at a binding energy of approximately 18.1 eV. The broad structure of this band suggests H_2O^+ is dissociative in the energy region of the band. The vibrational structure of this band is very complex with an erratic intensity pattern. Theoretical calculations [9] report that the B $^2B_2$ state of H_2O^+ has the same symmetry as the neutral ground

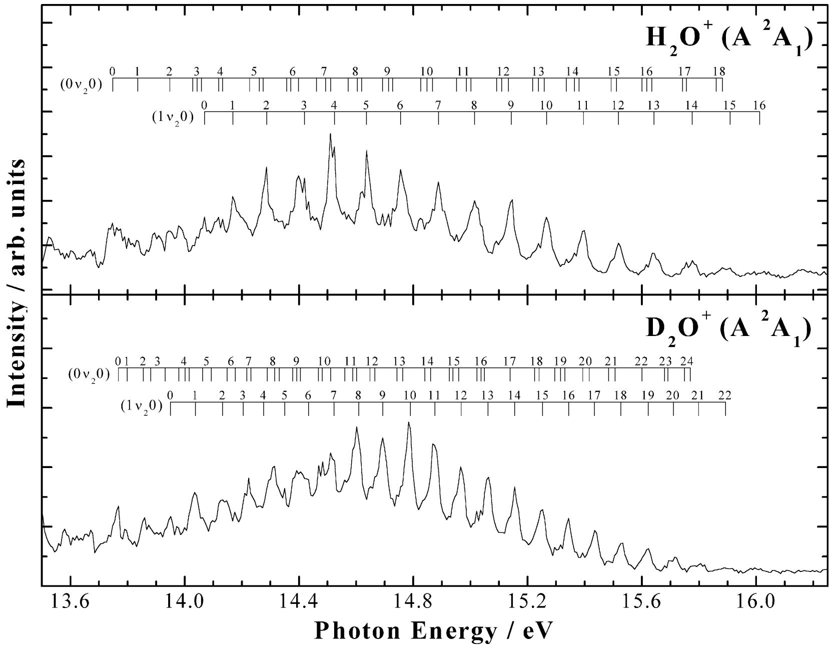

Fig. 4. Expanded views of a portion of the TPE spectra of H_2O and D_2O covering the A $^2A_1$ band system of H_2O^+ and D_2O^+ at an estimated energy resolution of ~7 meV. The spectra were recorded in 7 meV steps.

Table 6

Ionization energies (I.E.) (in eV), relative intensities and assignment of the vibrational transitions observed in the A $^2A_1$ band system of H_2O^+ and D_2O^+ from the present TPE work in comparison with a previous PE work.

Vibrational assignment ($v_1 v_2 v_3$)		Present work				Previous work[a]	
		H_2O^+		D_2O^+		I.E.	
		I.E.[b]	Intensity	I.E.[b]	Intensity	H_2O^+	D_2O^+
000		13.748	0.427	13.768	0.513		
010		13.835	0.314	13.798	0.356	13.8417	
020	Π	13.947	0.377	13.855	0.410	13.9388	13.8452
030	Γ	14.028	0.284				
030	Δ	14.043	0.337	13.881	0.373	14.0455	
030	Σ	14.058	0.389	13.931	0.359	14.0507	13.9309
100		14.069	0.462	13.950	0.446	14.0633	
040	G	14.118	0.463	13.979	0.371		
040	Φ	14.132	0.449	14.001	0.370	14.1410	13.9949
040	Π			14.016	0.454	14.1637	14.0091
110		14.168	0.590	14.037	0.497	14.1731	
050	Γ	14.227	0.385			14.2239	
050	Δ	14.260	0.478	14.062	0.450	14.2643	14.0755
050	Σ	14.275	0.637	14.093	0.407	14.2744	14.0889
120		14.287	0.780	14.132	0.556	14.2856	
060	G	14.356	0.419				
060	Φ	14.371	0.499	14.148	0.550	14.3652	14.1472
060	Π	14.398	0.725	14.176	0.474	14.3908	14.1688
130		14.419	0.709	14.204	0.529	14.4032	
070	Γ	14.460	0.460	14.217	0.586	14.4475	14.2163
070	Δ	14.493	0.544	14.231	0.594	14.5025	14.2430
070	Σ	14.511	1.000			14.5114	14.2532
140		14.524	0.911	14.276	0.425	14.5217	
080	G	14.572	0.498	14.289	0.639	14.5530	
080	Φ	14.603	0.510	14.314	0.764	14.6022	14.3140
080	Π	14.619	0.628	14.330	0.619	14.6398	14.3350
150		14.636	0.888	14.350	0.633	14.6519	14.3441
090	Γ	14.692	0.482	14.378	0.591		14.3708
090	Δ	14.713	0.479	14.392	0.729	14.7420	14.4081
090	Σ	14.727	0.515	14.405	0.719	14.7540	14.4231
160		14.755	0.768	14.433	0.690	14.7771	14.4360
0100	G	14.826	0.455	14.468	0.750		
0100	Φ	14.848	0.430	14.481	0.796	14.8470	14.5011
0100	Π	14.867	0.514	14.510	0.858	14.8749	14.5129
170		14.888	0.687	14.522	0.815	14.8905	14.5235
0110	Γ	14.951	0.352	14.560	0.582		
0110	Δ	14.986	0.387	14.588	0.775	14.9862	14.5817
0110	Σ	15.001	0.496	14.601	0.909	15.0010	14.6000
180		15.014	0.570	14.608	0.943	15.0154	14.6152
0120	G	15.091	0.310			15.0872	
0120	Φ	15.108	0.319	14.648	0.544	15.1130	14.6782
0120	Π	15.133	0.499	14.665	0.596	15.1303	14.6906
190		15.143	0.565	14.693	0.950	15.1400	14.7053
0130	Γ	15.217	0.237			15.2160	
0130	Δ	15.238	0.295	14.742	0.491	15.2380	14.7607
0130	Σ	15.257	0.422	14.763	0.551	15.2544	14.7785
1100		15.266	0.463	14.789	1.000	15.2679	14.7935
0140	G	15.335	0.198	14.840	0.566		
0140	Φ	15.364	0.234	14.860	0.641	15.3643	14.8591
0140	Π	15.380	0.295			15.3840	14.8727
1110		15.395	0.375	14.875	0.901	15.3942	
0150	Γ			14.926	0.359		
0150	Δ	15.492	0.184	14.938	0.448	15.4980	14.9357
0150	Σ	15.511	0.266	14.959	0.671	15.5101	14.9591
1120		15.518	0.299	14.967	0.726	15.5214	14.9677
0160	G	15.600	0.121	15.022	0.384		
0160	Φ	15.617	0.161	15.037	0.443	15.6256	15.0408
0160	Π	15.635	0.193	15.048	0.408	15.6437	15.0567
1130		15.642	0.193	15.061	0.682	15.6522	
0170	Γ	15.742	0.135			15.7356	15.0721
0170	Δ	15.756	0.176			15.7575	15.1294
0170	Σ			15.138	0.441	15.7720	15.1444
1140		15.775	0.186	15.155	0.638	15.7838	
0180	G	15.860	0.111	15.224	0.337	15.8595	15.2172
0180	Φ	15.882	0.122	15.240	0.423	15.8818	15.2336
0180	Π					15.9064	15.2449
1150		15.908	0.160	15.252	0.491		
0190	Γ			15.295	0.168	15.9875	
0190	Δ			15.315	0.186	16.0286	15.3217
0190	Σ			15.330	0.266	16.0402	15.3367
1160		16.012	0.108	15.344	0.345	16.0113	
0200	G			15.393	0.137		
0200	Φ			15.415	0.163		15.4205
0200	Π					16.1738	15.4316
1170				15.423	0.269	16.1384	15.4011
0210	Γ			15.483	0.083	16.2688	15.5102
0210	Δ			15.506	0.128		
0210	Σ					16.3054	15.5247
1180				15.525	0.199	16.2797	
0220	G						
0220	Φ			15.600	0.101		15.6092
0220	Π					16.4400	15.6215
1190				15.622	0.163	16.4010	
0230	Γ			15.679	0.057		
0230	Δ			15.691	0.101		15.6953
0230	Σ					16.5750	15.7170
1200				15.710	0.110	16.5320	15.7095
0240	G			15.749	0.037		
0240	Φ			15.769	0.055		
0240	Π						15.8123
1210				15.799	0.064	16.659	15.7979
1220				15.892	0.046		15.8927

[a] Reutt et al. [21].

[b] Uncertainty ±0.008 eV.

Table 7

Measured energies (in meV) of the v_1 and v_2 normal vibrational modes and calculated energy (in meV) of the v_3 normal vibrational mode and calculated force constants (in 10^5 dynes/cm) for the A $^2A_1$ state in H_2O^+ and D_2O^+.

Molecular ion	Normal vibrational mode energies			Force constants	
	hv_1	hv_2	hv_3	k_1	k_δ/l^2
H_2O^+	391 ± 21	112 ± 10	413 ± 3	5.80 ± 0.31	0.21 ± 0.50
D_2O^+	303 ± 10	57 ± 10	339 ± 1	7.04 ± 0.09	0.10 ± 0.03

state (C_{2v}). This state has a contracted equilibrium bond angle of 69° and a greater equilibrium bond length of 1.14 Å compared to 104.5° and 0.957 Å, respectively, for the neutral state [17]. Because of these changes in the molecular structure, it is expected that the symmetric bend and stretch normal modes, v_2 and v_1, will be strongly excited in this band. Brundle and Turner [4] first attempted to assign this band, suggesting that the vibrational structure consist of excitations of the normal modes v_1 and v_2. Also the slight decrease in v_1 and increase in v_2, compared with the values of the neutral ground state, suggests that an electron has been removed from an orbital with O–H bonding character and H–H antibonding character. This is because the removal of an electron from an orbital with O–H bonding character, would cause the bond length to increase and hence the bond vibration frequency to decrease and vice versa. Similarly, Karlsson et al. [6] and Reutt et al. [20] assigned different combinations of v_1 and v_2 to the vibrational structure of this band. However, Dixon et al. [7] suggested that the vibrational progression of this state consist of excitations of the v_1 and v_3 vibrations.

The intensities of the peaks at the beginning of the band system are very low, making it difficult to ascertain the adiabatic ionization energy of this band accurately. However, by extrapolation Brundle and Turner [4], Karlsson et al. [6] and Dixon et al. [7] have identified the adiabatic energy to be 17.22 eV, 17.189 eV and 17.183 eV, respectively. The B $^2B_2$ state of D_2O^+ is shown in an expanded view in the lower panel of Fig. 5. It has a similar structure to that of H_2O^+ (see upper panel of Fig. 5) with a sharp increase in

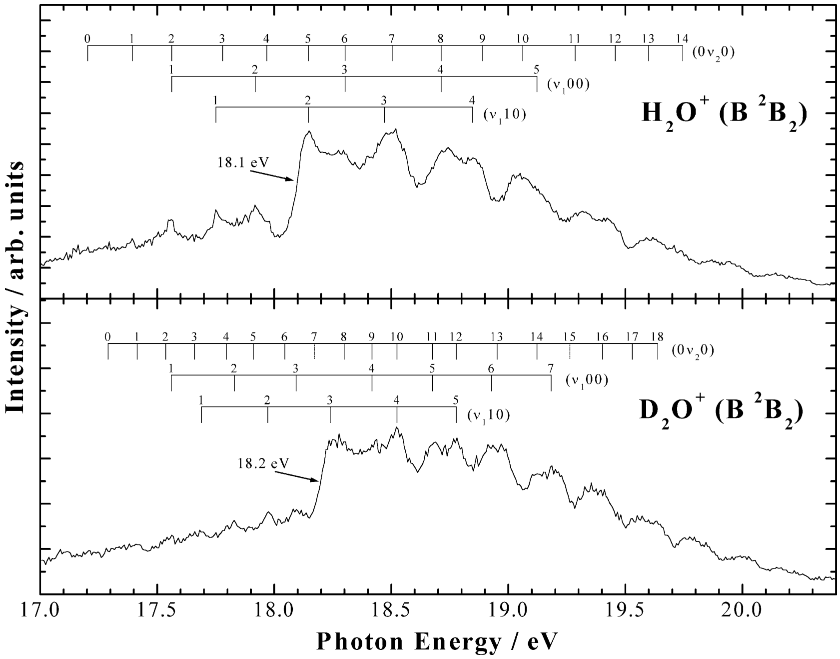

Fig. 5. Expanded views of a portion of the TPE spectra of H_2O and D_2O covering the B $^2B_2$ band system of H_2O^+ and D_2O^+ at an estimated energy resolution of ~9 meV. The spectrum was recorded in 7 meV steps. Note the unusual step-rise in the photoelectron yields (intensities) at ~18.1 eV and ~18.2 eV in H_2O^+ and D_2O^+, respectively.

the photoelectron yield at ~18.2 eV. Previously extrapolated values of the adiabatic energy for D_2O^+ are 17.26 eV and 17.272 eV by Brundle and Turner [4] and Karlsson et al. [6], respectively. Using the vibrational assignment of Karlsson et al. [6], the feature corresponding to the adiabatic ionization energy was identified to have an energy of 17.203 ± 0.008 eV (H_2O^+) and 17.290 ± 0.008 eV (D_2O^+).

From a preliminary assignment of the present data the values of v_1 and v_2 were determined for both H_2O^+ and D_2O^+. Knowing the energies of v_1 and v_2, the value of v_3 could be calculated [19]. A value of $\alpha = 34.5°$ for the half-bond angle was used [9], and in the process of calculating v_3, the values of the vibrational force constants k_1 and k_δ/l^2 were also calculated. The energies of the normal vibrational modes for the B $^2B_2$ state, for both molecules, are given in Table 8 together with the calculated values of the forces constants k_1 and k_δ/l^2. Because the vibrational structure in this band system is very complex, a tentative vibrational assignment was made for the main features only, using the normal modes v_1 and v_2. The results are given in Table 9 for H_2O^+ and Table 10 for D_2O^+. It should be noted that there appears to be more vibrational structure at the beginning of the B $^2B_2$ band system in D_2O^+ as compared to H_2O^+ and the order of the vibrational bands is different to that of H_2O^+ in some regions.

The most unusual feature within the TPE spectrum of H_2O is the sudden increase in the intensity within the B $^2B_2$ band system of H_2O^+ at ~18.1 eV and beyond (see the upper panel of Fig. 5). This intensity change is not seen in the PE spectrum of H_2O (see Fig. 2). Due to the broad structure of this band system in the PE spectrum, early experiments by Brundle and Turner [4] suggested that H_2O^+ is unstable in the B $^2B_2$ state, dissociating with a relatively short lifetime. According to measurements of Cottin [21], the threshold for OH^+ production from H_2O is at 18.1 eV, measured using the electron impact TOF method. The coincidence in the energy of the sharp increase in the photoelectron yield seen in the TPE spectrum with the appearance energy of the fragment ion OH^+ suggests that a link exists between the production of threshold electrons and the formation of OH^+. Stockbauer [22] utilized a photoelectron-photoion coincidence mass spectrometer to ob-

Table 8
Measured energies (in meV) of the v_1 and v_2 normal vibrational modes and calculated energy (in meV) of the v_3 normal vibrational mode and calculated force constants (in 10^5 dynes/cm) for the B $^2B_2$ state in H_2O^+ and D_2O^+.

Molecular ion	Normal vibrational mode energies			Force constants	
	$h\nu_1$	$h\nu_2$	$h\nu_3$	k_1	k_δ/l^2
H_2O^+	360 ± 10	190 ± 10	352 ± 7	4.57 ± 0.69	0.67 ± 0.21
D_2O^+	272 ± 10	124 ± 10	261 ± 1	4.83 ± 0.23	0.55 ± 0.11

Table 9
Ionization energies (I.E.) (in eV), relative intensities and tentative assignment of the vibrational transitions observed in the B $^2B_2$ band system of H_2O^+ from the present TPE work in comparison with a previous PE work.

Vibrational assignment ($v_1 v_2 v_3$)	Present work		Previous work[a]
	I.E.[b]	Intensity	I.E.
000	17.203	0.310	17.189
010	17.393	0.359	17.378
100/020	17.562	0.463	17.552
110	17.750	0.525	17.746
030	17.779	0.468	17.915
200	17.919	0.550	18.134
040	17.968	0.454	
210/050	18.145	0.974	
300/060	18.302	0.860	
310	18.470	0.969	
070	18.503	1.000	
400/080	18.712	0.869	
410	18.847	0.825	
090	18.890	0.820	
0100	19.061	0.723	
500	19.121	0.614	
0110	19.285	0.517	
0120	19.456	0.446	
0130	19.599	0.348	
0140	19.744	0.235	

[a] Karlsson et al. [6].
[B] Uncertainty ±0.008 eV.

Table 10
Ionization energies (I.E.) (in eV), relative intensities and tentative assignment of the vibrational transitions observed in the B $^2B_2$ band system of D_2O^+ from the present TPE work in comparison with a previous PE work.

Vibrational assignment ($v_1v_2v_3$)	Present work		Previous work[a]
	I.E.[b]	Intensity	I.E.
000	17.290	0.276	17.272
010	17.414	0.308	17.412
020	17.536	0.330	17.550
100	17.560	0.360	17.693
030	17.660	0.383	
110	17.689	0.377	
040	17.796	0.412	
200	17.829	0.450	
050?	17.911	0.404	
210	17.972	0.495	
060?	18.045	0.466	
300	18.093	0.519	
310	18.239	0.942	
080	18.298	0.921	
400/090	18.417	0.919	
410/0100	18.524	1.000	
500/0110	18.678	0.924	
510/0120	18.777	0.956	
600	18.928	0.901	
0130	18.952	0.901	
0140	19.122	0.749	
0160	19.402	0.589	
0170	19.529	0.392	
0180	19.637	0.362	

[a] Karlsson et al. [6].
[b] Uncertainty ±0.008 eV.

tain data on the production of OH^+ ions from H_2O^+. They also measured a TPE spectrum of H_2O in the region of the B $^2B_2$ state that displayed a similar step in the intensity profile at ~18.1 eV as observed here. It was also found that at the onset of OH^+ production at ~18.1 eV, the intensity of the parent ion H_2O^+ decreased to nearly zero as the intensity of the OH^+ fragment increased to a value ~60% greater than that of H_2O^+ below the step. Because it is reasonable to expect that the same process(es) occur in D_2O, the TPE spectrum of D_2O should prove to be instructive. As expected, (see the lower panel of Fig. 5), the TPE spectrum of D_2O also shows a sudden increase in the intensity within the B $^2B_2$ band system at around the same energy (~18.2 eV) and beyond as that for H_2O. This energy is comparable to the appearance energy of OD^+ at 18.18 eV measured at room temperature by Dibeler et al. [23]. The dissociation energy of D_2O^+ into OD^+ is slightly higher than that for H_2O^+ into OH^+, due to the fact that D_2O is heavier than H_2O (zero-point energy effect).

Eland [24] carried out coincidence measurements on D_2O, using a time-of-flight coincidence mass spectrometer, and measured the yield of D_2O^+ and OD^+ ions in the energy region of the B $^2B_2$ state. The production of D_2O^+ (by vertical transitions) was found in the energy regions of the X $^2B_1$ and A $^2A_1$ states, and also within the energy region of the first few vibronic levels of the B $^2B_2$ state. However, it was found that as soon as the photon energy is high enough OD^+ is produced, and its yield increases as the yield of D_2O^+ decreases.

Hence, it is widely accepted that H_2O^+ dissociates to produce OH^+ at the onset of the OH^+ threshold. However, the increase in the production of threshold electrons caused by fragmentation of the water molecule is not fully understood. Fiquet-Fayard and Guyon [25] have calculated the potential energy curves for H_2O and suggests that the B $^2B_2$ state of H_2O^+ is completely predissociated by curve crossing with the repulsive $^4A''$ state to give OH^+. Assuming that OH^+ is produced by predissociation of H_2O^+, there have also been suggestions that this predissociation process is in direct competition with a second process [22]. This second process could be autoionization of excited states of H_2O (H_2O^*) in the same energy region. According to Dutuit et al. [16], there exist excited states of H_2O in the energy region 16–19 eV, due to the excitation of the $1b_2$ electron. Since it is more likely that excited states of H_2O are accessed using the TPE method, the autoionization of these states would produce an increase in the yield of threshold photoelectrons. Assuming that predissociation and autoionization occur with approximately the same probability at and above the onset, Stockbauer [22] proposed that if the rate at which predissociation occur increases, then the rate of autoionization would also increase. This would cause the observed sudden increase in the yield of threshold photoelectrons.

The fact that the onset is seen in the TPE spectrum and not seen in the PE spectrum supports the suggestion of Stockbauer [22], since the indirect processes of predissociation and autoionization are less likely to be detected using the PES technique. This also suggests that the enhanced onset of threshold electrons at ~18.1 eV is not due to direct ionization of H_2O, but is due to autoionization. These autoionization effects would not have been readily detected in the previous experiments using electron impact methods and in photoionization experiments detecting finite energy electrons.

3.6. The $(2a_1)^{-1}$ state of H_2O^+ and D_2O^+

The fourth band system seen in the TPE spectra of H_2O and D_2O (see the upper and lower panels in Fig. 1, respectively) arises from the ionization of an inner valence electron from the $2a_1$ molecular orbital. The $2a_1$ orbital contains mostly oxygen (2s) atomic orbital character and so it is mainly atomic in character accounting for its structureless feature, except for a broad shoulder on the lower binding energy side of the peak assigned to the $(2a_1)^{-1}$ state, with an onset energy of ~25 eV. Because the band system is quite simple it was straightforward to fit two Gaussian peaks to the two features as shown in Fig. 6 for H_2O^+. From the fitted peaks, the vertical ionization energy of the feature assigned to the $(2a_1)^{-1}$ state was found to be ~32.3 eV and the vertical ionization energy of the shoulder was found to be ~27.6 eV. The results for D_2O^+ were the same within the experimental error. The ionization energy of the $(2a_1)^{-1}$ state lies just below the double ionization energy of H_2O, which has a theoretical value of 36.93 eV [26]. The $(2a_1)^{-1}$ band system of H_2O^+ has been measured in the past by Potts and Price [5], who used a HeII light source to measure the photoelectron spectrum of H_2O. From their data they determined the vertical ionization energy of the $(2a_1)^{-1}$ state to be equal to 32.2 eV, which is in agreement with the value obtained in the present work.

It is well known from theoretical calculations that ionization of inner-valence states, for most molecules, results in the breakdown of the independent-particle approximation, as discussed by Cederbaum et al. [27]. Thus, in the inner-valence region, there is usually a high density of satellite states. These are excited ionic states involving the excitation of a valence electron simultaneously with the ionization of a core electron. These states are also referred to as configuration interaction (CI) states. The correlation of the core ionic state with these satellite states will cause a redistribution of the 'main-line' intensity of the core ionic state amongst these satellite states. This leads to the broadening of the band. As a result, these satellite states do not only appear at energies greater than the 'main-line', but at lower energies as well [27]. The latter may be due to quasi-degeneracy between the inner valence single-hole ionic state and the two-hole-one-particle configuration of the satellite state as discussed by Yencha et al. [28].

Martensson et al. [29] measured the inner-valence electron spectrum of gaseous H_2O using the Electron Spectroscopy for Chemical Analysis (ESCA) technique. They detected several CI resonance structures in the valence spectrum, especially near the

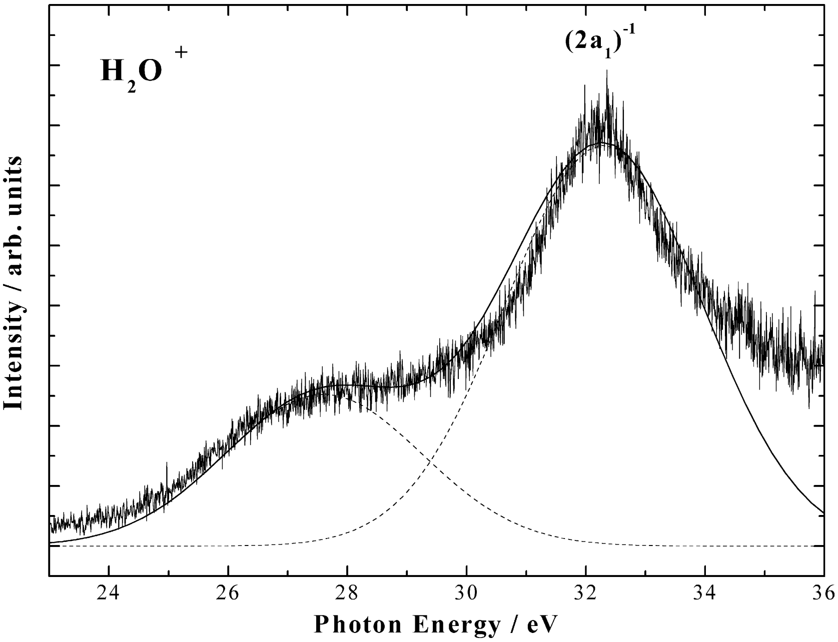

Fig. 6. An expanded view of a portion of the TPE spectrum of H_2O covering the $(2a_1)^{-1}$ inner valence ionization region of H_2O. Gaussian peaks are fitted to the two discernible features in the region allowing for the determination of the peak energy positions of the features.

$(2a_1)^{-1}$ band system, one of which corresponds to the transition $(1b_1)^1 4a_1^*$ at an energy of 27 eV. This agrees with the value of the satellite state at 27.02 eV calculated by Cederbaum [30] using Green's functions. Wood [31] investigated the 'shake-up' peaks (satellite states) of H_2O in the inner-valence region using CI techniques. He found eleven states in the energy region 17.6–29.7 eV, one of which included a state at 27.1 eV. This value agrees with the value obtained by Martensson et al. [29] and Cederbaum [30]. The calculated satellite state at around 27 eV [29–31] compares well with the energy of the shoulder on the $(2a_1)^{-1}$ line in the present TPE spectrum. This shoulder is therefore assigned to the $(1b_1)^1 4a_1^*$ resonant state, following the assignment used by Martensson et al. [29].

Tan et al. [32] used electron-impact coincidence techniques to measure the cross-sections for photo-processes and fragmentation in H_2O. They also obtained a PE spectrum for H_2O, at a photon energy of 41 eV, and observed the $(2a_1)^{-1}$ band system. This suggests that the $(2a_1)^{-1}$ state can be accessed directly, and is not dependent on autoionization effects. Their results showed that H_2O^+ in the $(2a_1)^{-1}$ state dissociates completely, producing H^+ and O^+. This would add to the reason for the broad structure of the band and the lack of any visible vibrational structure, since the state is highly repulsive.

4. Summary

Complete threshold photoelectron (TPE) spectra of H_2O and D_2O up to 40 eV binding energy are presented for the first time at a resolution varying smoothly from ~6 meV at 12 eV photon energy to ~20 meV at 40 eV photon energy. Analysis of the TPE spectrum of H_2O by comparison with the measured (0.5 eV) constant-kinetic-energy photoelectron (PE) spectrum of H_2O reveals major differences in the appearance of the observed bands of H_2O^+ in the outer valence ionization region (12–20.5 eV). These differences include (1) the 'filling-in' in between the band systems in the Franck–Condon gap regions in the TPE spectrum, (2) in the shifting of the maximum in the band intensity of the second and third band systems towards lower energy in the TPE spectrum, and (3) in an abrupt increase in the photoelectron yield at ~18.1 eV in the third band system in the TPE spectrum. These features are mirrored in the TPE spectrum of D_2O. All of these differences are attributed to the autoionization of Rydberg states residing across the entire photon energy region. These Rydberg states appear to be major contributors to the TPE spectrum. Specifically, in the ground state of the cations, four vibrational progressions were observed while only two were identified in past photoelectron studies. For the A $^2A_1$ state the Renner–Teller effect was considered as a cause for the splitting of the vibrational levels building on the work of Reutt et al. [20]. The adiabatic ionization energies of the A $^2A_1$ state for both molecules were determined from the TPE spectra. Also some previously unassigned vibrational levels were measured for this state. The third state (B $^2B_2$) has a very complex vibrational structure and has not been consistently assigned by previous experimenters. However, from the TPE spectra, the main vibrational states have been tentatively assigned here using a combination of the v_1 and v_2 normal modes. The unusual step-rise in the photoelectron yield within the third band system at ~18.1 eV in H_2O^+ and the simultaneous production of OH^+ ions at the same energy, with an equally enhanced ion intensity compared with the H_2O^+ intensity just below the threshold energy of OH^+, strongly suggests that both phenomenon result from the enhanced production of H_2O^+ ions by autoioniztion of Rydberg states producing threshold electron, and sequentially, by the rapid predissociation of H_2O^+, the production of OH^+ ions.

In the inner-valence ionization region studied (25–40 eV) the TPE spectra of H_2O and D_2O display a broad structureless feature assigned as the $(2a_1)^{-1}$ 'main-line' state with a peak maximum binding energy of ~32.3 eV and a should with a peak maximum binding energy of ~27.6 eV that is assigned as the $(1b_1)^1 4a_1^*$ resonant state. The broadness of the inner valence states suggests that they are highly repulsive adding to the broadness due to CI effects.

This study demonstrates how threshold photoelectron spectroscopy affords a different perspective of the photoionization of molecules as compared to conventional photoelectron spectroscopy and is a means of gaining additional information about the electronic states of ions.

Acknowledgements

The authors thank the CLRC Daresbury Laboratory for providing beam time and facilities for carrying out this study. Financial support for this research from the Engineering and Physical Sciences Research Council (UK) (EPSRC) is gratefully acknowledged.

References

[1] H.J. Henning, Ann. Phys. 13 (1932) 599.
[2] W.C. Price, J. Chem. Phys. 4 (1936) 147.
[3] M.I. Al-Joboury, D.W. Turner, J. Chem. Soc. B (1967) 373.
[4] C.R. Brundle, D.W. Turner, Proc. Roy. Soc. A 307 (1968) 27.
[5] A.W. Potts, W.C. Price, F.R.S, Proc. Roy. Soc. A 326 (1972) 181.
[6] L. Karlsson, L. Mattsson, R. Jadrny, R.G. Albridge, S. Pinchas, T. Bergmark, K. Siegbahn, J. Chem. Phys. 62 (1975) 4745.
[7] R.N. Dixon, G. Duxbury, J.W. Rabalais, L. Åsbrink, Mol. Phys. 31 (1976) 423.
[8] H. Lew, Can. J. Phys. 54 (1976) 2028.
[9] J.C. Leclerc, J.A. Horsely, J.C. Lorquet, Chem. Phys. 4 (1974) 337.
[10] C.F. Jackels, J. Chem. Phys. 72 (1980) 4873.
[11] A.J. Yencha, G. Dujardin, A. Hopkirk, A. Kvaran, R.J. Donovan, G.C. King, L. Heller, M.J. Besnard-Ramage, R.R. Maier, S. Spyrou, Book of Abstracts, XVIII ICPEAC, Aarhus, Denmark, 1993, p. 88.
[12] R.I. Hall, A. McConkey, K. Ellis, G. Dawber, L. Avaldi, M.A. MacDonald, G.C. King, Meas. Sci. Technol. 3 (1992) 316.
[13] S. Cvejanovic, F.H. Read, J. Phys. B: Atom. Mol. Phys. 7 (1974) 118.
[14] G.C. King, G. Dawber, Selected Topics on Electron Physics, Plenum Press, New York, 1996.
[15] A.J. Yencha, A. Hopkirk, A. Hiraya, G. Dujardin, A. Kvaran, L. Heller, M.J. Besnard-Ramage, R.J. Donovan, J.G. Goode, R.R.J. Maier, G.C. King, S. Spyrou, J. Electron Spectrosc. Relat. Phenom. 70 (1994) 29.
[16] O. Dutuit, A. Tabche-Fouhaile, I. Nenner, H. Frohlich, P.M. Gyon, J. Chem. Phys. 83 (1985) 584.
[17] G. Herzberg, Electronic Spectra of Polyatomic Molecules, Van Nostrand Reinhold Co. Ltd., Princeton, New Jersey, 1966. p. 585.
[18] A.J. Yencha, A.J. Cormack, R.J. Donovan, A. Hopkirk, G.C. King, Chem. Phys. 238 (1998) 109.
[19] G. Herzberg, Infrared and Raman Spectra of Polyatomic Molecules, Van Nostrand Reinhold Co. Ltd., Princeton, New Jersey, 1945. p. 169.
[20] J.E. Reutt, L.S. Wang, Y.T. Lee, D.A. Shirley, J. Chem. Phys. 85 (1986) 6928.
[21] M. Cottin, J. Chem. Phys. 56 (1959) 1024.
[22] R. Stockbauer, J. Chem. Phys. 72 (1980) 5277.
[23] V.H. Dibeler, J.A. Walker, J. Rosenstock, J. Res. Nat. Bur. Stand. US 70A (1966) 197.
[24] J.H.D. Eland, Chem. Phys. 11 (1975) 41.
[25] F. Fiquet-Fayard, P.M. Guyon, Mol. Phys. 11 (1966) 17.
[26] T.J. Van Huis, S.S. Wesolowski, Y. Yamaguchi, H.F. Schaefer III, J. Chem. Phys. 110 (1999) 11856.
[27] S. Cederbaum, J. Domcke, J. Schirmer, Phys. Scr. 21 (1980) 481.
[28] A.J. Yencha, M.C.A. Lopes, M.A. MacDonald, G.C. King, Chem. Phys. Lett. 310 (1999) 433.
[29] N. Martensson, P.A. Malmquist, S. Svensson, E. Basilier, J.J. Pireaux, U. Gelius, K. Siegbahn, Nouveau J. Chim. 1 (1977) 191.
[30] S. Cederbaum, Ph.D. Thesis, University of Munich, 1972.
[31] M. Wood, Chem. Phys. 5 (1974) 471.
[32] K.H. Tan, C.E. Brion, Ph.E. Van Der Leeuw, M.J. Van Der Wiel, Chem. Phys. 29 (1978) 299.